

Effect of calcium enrichment of Cheddar cheese on its structure, in vitro digestion and lipid bioaccessibility

Erik Ayala-Bribiesca^{a,b}, Martine Lussier^b, Denise Chabot^c, Sylvie L. Turgeon^a, Michel Britten^{b,*}

^a *Institute of Nutrition and Functional Foods (INAF) and Dairy Science and Technology Research Centre (STELA), Department of Food Sciences and Nutrition, Pavillon Paul-Comtois, Laval University, Sainte-Foy, Quebec, Canada, G1V 0A6*

^b *Food Research and Development Centre, Agriculture and Agri-Food Canada, 3600 Casavant Boulevard West, Saint-Hyacinthe, Quebec, Canada, J2S 8E3*

^c *Eastern Cereal and Oilseed Research Centre, Agriculture and Agri-Food Canada, 960 Carling Avenue, Ottawa, Ontario, Canada, K1A 0C6*

*Corresponding author

Tel.: 450-773-1105

Fax: 450-773-8461

E-mail address: michel.britten@agr.gc.ca

1 ABSTRACT

2

3 The nutritional role of cheese is usually reduced to its composition, often neglecting the effect
4 that the matrix can have on digestion. The purpose of this study was to establish a link between
5 the characteristics of Cheddar cheeses with different calcium levels and the impact on cheese *in*
6 *vitro* digestion. Curds were enriched with CaCl₂ during the salting step to produce control, high-
7 calcium, and very high-calcium cheeses. Cheese composition, texture and structure were
8 characterized, and physical disintegration and lipolysis were monitored during *in vitro* digestion.
9 Cheese hardness increased with higher calcium content. This resulted in a slower disintegration
10 during *in vitro* digestion. Despite showing faster disintegration, the control cheese had the
11 slowest lipolysis progression. The results suggest that lipolysis depends on calcium content and
12 the matrix modulating the access of enzymes to their substrates. Further studies should provide a
13 better understanding of the calcium-matrix interaction affecting lipid bioaccessibility.

14

15 **1. Introduction**

16

17 When food enters the human body, digestion takes place to release the nutrients from the
18 matrix so that they can be absorbed. The mechanical characteristics and intrinsic composition of
19 the matrix influence the entire digestion process by controlling the matrices' disintegration and
20 biochemical behavior under gastrointestinal conditions (Hur, Lim, Decker, & McClements, 2011;
21 McClements, Decker, & Park, 2009). Hence, the food matrix acts as a nutrient-release regulator
22 as the matrix disintegrates during the digestion process (Turgeon & Rioux, 2011), thus

23 determining nutrient bioaccessibility, which is defined as the fraction of a substance that is
24 soluble in the gastrointestinal environment and is available for absorption (Ruby et al., 1999).

25 Among nutrients, lipids demand a more complex digestion and absorption strategy than
26 water-soluble substances (Klein, Cohn, &Alpers, 2006). Dietary lipids are composed mainly of
27 triacylglycerols. After being released from the matrix, the triacylglycerol-rich fat droplets are
28 exposed to lipases which cleave the ester bonds on the glycerol backbone, releasing free fatty
29 acids. Fatty acids and other fat-soluble components must be incorporated into mixed micelles
30 and transported to the enterocyte brush border for absorption (Jones &Kubow, 2006). Therefore,
31 lipid bioaccessibility may be estimated from the amount of lipids transferred into the aqueous
32 micellar fraction (Failla&Chitchumronchokchai, 2005). Several studies have shown that
33 emulsion characteristics may affect lipase activity, an effect that is explained mainly by the
34 accessibility to the triacylglycerols (Armand et al., 1999; Clemente et al., 2003; Favé, Coste, &
35 Armand, 2004; McClements et al., 2009; Michalski, Briard, Desage, & Geloën, 2005). Extensive
36 studies on emulsion engineering have provided a basic overview of digestion mechanisms
37 (McClements et al., 2009; Singh, Ye, & Horne, 2009), but because those studies are not entirely
38 applicable to edible food systems, further research on actual foods is needed.

39 In dairy products, a wide array of matrices can be found, and an increasing number of
40 studies report that the physical structure of milk-fat-rich foods modifies the way lipids are
41 digested and absorbed (Clemente et al., 2003; Lopez &Gaucheron, 2008). Besides lipids, a key
42 nutrient associated with dairy foods is calcium. Calcium is known to interact with milk
43 components, influencing the structural properties of dairy matrices such as cheese (Lucey & Fox,
44 1993). Furthermore, calcium has been reported to enhance lipolysis during digestion by
45 precipitating free fatty acids in the intestinal medium, a process that in turn may reduce

46 bioaccessibility (Lopez & Gaucheron, 2008; Lorenzen et al., 2007; McClements et al., 2009).
47 This reduction occurs because fatty acids, as lipolysis products, accumulate at the lipid–water
48 interface and limit the access of lipase to its substrates (Favé et al., 2004). Calcium enhances
49 lipolysis by removing fatty acids from the interface in the form of calcium soaps, which are not
50 water-soluble under intestinal conditions (Hu, Li, Decker, & McClements, 2010). Insolubility
51 limits fatty-acid bioaccessibility and translates into reduced absorption (Lorenzen et al., 2007).

52 Cheese is a complex matrix of milk proteins (mainly casein), fat, minerals, and water, where
53 casein forms the major structural network and entraps the fat (Mistry & Anderson, 1993).
54 Roughly speaking, protein contributes to hardness, and fat and water contribute to smoothness
55 (Metzger & Mistry, 1994, 1995). The protein network determines the rheological properties of
56 cheese, mainly due to calcium-casein interactions and proteolysis, which contribute significantly
57 to the textural properties (Lucey, Johnson, & Horne, 2003). Among Cheddar cheeses (pH between
58 4.9 and 5.4), higher mineral levels result in cheeses with a harder texture, as compared to
59 Cheddar cheeses with lower mineral levels (Lucey & Fox, 1993; Metzger & Mistry, 1994, 1995).
60 The rheological properties of cheese also depend on the size distribution and membrane
61 composition of fat globules (Michalski, Michel, & Geneste, 2002). In cheese, partially coalesced
62 fat globules may lead to the formation of large fat aggregates, which are non-globular inclusions
63 of milk fat that result from the disruption of individual milk-fat globules, so that lipids can fill
64 voids in the protein matrix (Michalski et al., 2007). Such fat aggregates occur mainly during the
65 manufacturing process, when the warm curd is cheddared, and these influence the textural
66 properties of the cheese (Guinee, Auty, & Fenelon, 2000).

67 Cheddar cheese is suitable for studying the impact of the food matrix on lipid
68 bioaccessibility. Modifying the microstructure of the matrix could alter the way the matrix itself

69 is digested. For example, it is reasonable to postulate that a harder matrix will resist breakdown
70 and delay nutrient release. In Cheddar cheese, increasing the amount of calcium strengthens the
71 protein matrix and could lead to a delayed disintegration in the digestive system. The dissolution
72 of food matrices will depend on water absorption and diffusion of acid and enzymes (Van Wey
73 et al., 2014). The rate of fat release during digestion may result in different bioaccessibility
74 profiles, as previously observed for different types of cheese (Lamothe, Corbeil, Turgeon, &
75 Britten, 2012).

76 The evolution of the cheese matrix during the first weeks of ripening could impact the way
77 the matrix behaves during digestion. During ripening, cheese structure evolves mainly because of
78 proteolysis and colloidal calcium solubilization (Johnson & Lucey, 2006; O'Mahony, Lucey,
79 &McSweeney, 2005). Proteolysis is one of the factors that may modify the texture of young (or
80 mild) Cheddar cheese by softening the para-casein network (Guinee et al., 2000; Lawrence et al.,
81 2004; O'Mahony et al., 2005), but the most important factor that modifies Cheddar cheese
82 texture during the first weeks of ripening is the level of calcium, namely in the form of colloidal
83 calcium phosphate (CCP). CCP is the insoluble part of calcium and phosphate attached to the
84 protein matrix in a colloidal form (Lucey & Fox, 1993; O'Mahony, McSweeney, & Lucey,
85 2006). By strengthening the para-casein matrix, CCP acts as a structuring element (Hassan,
86 Johnson, & Lucey, 2004). In Cheddar cheese, CCP greatly decreases during the first 21 d of
87 ripening and is highly correlated with texture softening during the same period (O'Mahony et al.,
88 2005). In sum, physicochemical events that modify the texture of cheese may have an impact on
89 the resistance of the cheese matrix to digestion.

90 It has been shown that the characteristics of the food matrix influence the kinetics of
91 digestion and nutrient bioaccessibility (Ellis et al., 2004; Hornero-Méndez & Mínguez-Mosquera,

92 2007; Lopez & Gaucheron, 2008), but such processes are still poorly understood. Modifying
93 cheese microstructure and composition through technological processing could modulate the
94 bioaccessibility of lipids. The purpose of this study was to examine the effect of calcium
95 enrichment and short-term ripening on Cheddar cheese structure and to assess the impact of that
96 structure on lipid bioaccessibility.

97

98 **2. Materials and methods**

99

100 *2.1. Preparation of Cheddar-type cheeses*

101

102 One standardized batch of Cheddar curd was produced in a pilot plant (Food Research and
103 Development Centre, Saint-Hyacinthe, QC, Canada) from whole pasteurized milk
104 (Laiterie Chalifoux, Sorel, QC, Canada). The milk was warmed to 32°C. A commercial starter
105 (CH-FRS-102 culture; Chr. Hansen, Hørsholm, Denmark) and 0.26 mL kg⁻¹ of 45% w/v CaCl₂
106 solution (Cal-Sol; Fromagex, Rimouski, QC, Canada) were added. After 1 h, 0.085 mL kg⁻¹ of
107 microbial chymosin solution (ChyMax; Chr. Hansen) was added. Once set, the gel was cut and
108 then cooked by increasing the temperature to 38°C at a rate of 0.2°C min⁻¹. The whey was
109 drained when the pH reached 6.0. The curd was cheddared for 1 h and milled when the pH
110 reached 5.1. The milled curds were separated into three batches and salted with NaCl and
111 CaCl₂·2H₂O (Sigma-Aldrich, Oakville, ON, Canada) in the amounts shown in Table 1 to obtain
112 the different Cheddar-type cheeses. The curds were then packed into 13-kg-capacity stainless
113 steel molds lined with synthetic cheesecloth and pressed at room temperature for 1 h at 275 kPa.
114 The cheeses were removed from the molds, vacuum-packed, and kept at 4°C. After 1 week, one

115 third of each cheese was cut into 300-g blocks, which were then individually vacuum-packed and
116 frozen at -20°C until required for the experiments. The same was done with another third after
117 2 weeks and the last third after 4 weeks. The cheeses were thawed at 4°C for 4 d before the
118 experiments to allow the matrix to stabilize and to limit the crumbly texture that has been
119 reported in Cheddar cheeses after a freeze–thaw cycle (Kasprzak, Wendorff, & Chen, 1994).

120

121 *2.2. Cheese composition*

122

123 All reagents were obtained from Fisher Scientific (Ottawa, ON, Canada) unless otherwise
124 specified. Moisture was quantified by difference from total solids, obtained by oven-drying 1 g
125 of cheese in an aluminum cup at 100°C for 16 h. Protein ($\text{N}\times 6.38$) was quantified by the
126 Kjeldahl method (AOAC, 1995a). Fat was quantified by the Mojonnier method (AOAC, 1995b).
127 Dry samples were incinerated in a muffle furnace at 550°C for 16 h, and the residues were
128 weighed to determine ashes. Cheese pH was measured in a slurry prepared with 10 g of cheese
129 and 10 g of distilled water.

130 The cheese ashes were dissolved in 0.23 M HNO_3 and used to quantify calcium by
131 inductively coupled plasma–optical emission spectroscopy with a Teledyne Leeman Prism
132 spectrometer (010-00084-1; Hudson, NH, USA). Commercial standards (Fisher Scientific) were
133 diluted in the same solution. Detection was done in radial mode on the argon plasma torch.

134 Colloidal calcium (CCP) was determined by acid–base titration (pH 7 to 3) and back-
135 titration (pH 3 to 7), in accordance with a previous study (Rémillard & Britten, 2011). The
136 results were reported as mg of calcium per g of protein (mg g^{-1}).

137 To monitor proteolysis during the ripening period, water-soluble nitrogen in the cheeses was
138 determined (Christensen, Bech, & Werner, 1991). Cheese slurries were prepared in distilled
139 water (2:1 water-to-cheese ratio). The slurries were kept at 40°C for 1 h and then centrifuged for
140 30 min at $3010 \times g$ and 4°C. The aqueous phase was filtered, and the solids were extracted once
141 again. The nitrogen in the pooled aqueous phases was quantified by the Kjeldahl method. The
142 results were reported as a percentage of water-soluble nitrogen with respect to total nitrogen (%
143 WSN TN⁻¹).

144

145 *2.3. Texture profile analysis*

146

147 A texture profile analysis (TPA) was carried out to evaluate the impact of calcium
148 supplementation on cheese texture. Cylindrical samples ($r = 5 \text{ mm}$; $h = 10 \text{ mm}$) were cut at 4°C
149 and stored for 30 min at 22°C. A double compression cycle to a 30% strain with a Plexiglas
150 probe moving at a rate of 0.4 mm s^{-1} rate was done using a TA-XT2 texture analyzer equipped
151 with a 5-kg load cell (Stable Micro Systems, Surrey, UK) and Exponent software
152 (version 6.1.4.0; Stable Micro Systems). Hardness, springiness, and cohesiveness were computed
153 from the TPA data (Tunick, 2000). The TPA was done in triplicate, and each sample was
154 composed of 10 cheese cylinders. Outliers, more than two standard deviations from the average
155 maximum force during the first compression, were omitted from the data analysis.

156

157 *2.4. Scanning electron microscopy*

158

159 The cheeses were cut into sticks measuring $3 \times 3 \times 7$ mm with a razor blade. The sticks were
160 immediately covered with a protein-fixation buffer (pH 7.2) containing 2% glutaraldehyde
161 (18426; Ted Pella, Redding, CA, USA) in 0.1 M sodium cacodylate (Sigma-Aldrich) and then
162 fixed for 2 h at 21°C under gentle agitation. The protein-fixation buffer was removed, and the
163 sticks were dehydrated in a graded series of ethanol concentrations (30%, 50%, 70%, 80%, 90%,
164 95%, and twice in 100%), each for 15 min under gentle agitation. The samples were then
165 defatted three times with hexane under the same agitation conditions. The samples were freeze-
166 fractured in liquid nitrogen, dried in carbon dioxide with a critical point dryer (Biodynamics
167 Research Corp., Rockville, MD, USA), and mounted on aluminum stubs. The mounted samples
168 were covered with a 10-nm layer of gold using an Emitech K550X sputter coater (Quorum
169 Technologies, Kent, UK). Scanning electron micrographs were obtained with an ESEM XL-30
170 microscope (Philips, Eindhoven, the Netherlands) operating under high vacuum at 5 kV, with a
171 secondary electron detector with an HD filter, a spot size of 3, and a working distance of 7 to
172 10 mm. At least 15 fields of each cheese were observed, and typical fields were imaged. Fields
173 showing curd junctions were discarded.

174

175 *2.5. Confocal laser microscopy*

176

177 The cheeses were cut on a refrigerated surface into 3-mm cubes and frozen in an isopentane
178 bath cooled in liquid nitrogen. Slices (20- μ m thick) were cut using a microtome (Reichert Jung,
179 Wetzlar, Germany) at -27°C . Each slice was mounted on a microscope slide with an adhesive

180 marker (Fro-Tissuer, 22302; Ted Pella) allowed to dry for 10 min at -18°C , and stained with a
181 drop of 0.01% aqueous solution of Nile Blue A (Sigma-Aldrich) for 15 min over ice. The use of
182 Nile Blue A allows simultaneous staining of fat and protein (Auty, Twomey, Guinee,
183 & Mulvihill, 2001). With the microscope slide still being on ice, each sample was rinsed, the
184 excess water was removed, and the sample was mounted with Fluoromount G and observed
185 under a Zeiss Meta-510 confocal microscope equipped with a Plan Apochromat $40\times$ objective
186 with a numerical aperture of 1.4 (Carl Zeiss GmbH, Jena, Germany). Fat and protein were
187 detected, respectively, with an Argon/2 laser, line 488 nm for excitation and band-pass 530-to-
188 600-nm emission, and with a HeNe laser, line 633 nm for excitation and long-pass 650-nm
189 emission. The slides were kept over a refrigerated surface during observation to reduce fat
190 mobility. The images were processed with Zen software (version 2009; Carl Zeiss GmbH). The
191 pseudo-colors chosen were green for fat and red for protein, and both images were superimposed
192 to show the relative distribution of fat and protein. At least five samples of each cheese were
193 observed, and typical images were captured. Images showing curd junctions were discarded.

194

195 2.6. *In vitro* digestion of Cheddar-type cheeses

196

197 The *in vitro* digestion model and fluid composition simulating the physicochemical
198 conditions of human digestion during the fed state (Versantvoort, Oomen, Van de Kamp,
199 Rompelberg, & Sips, 2005) were adapted for the digestion of cheese. Briefly, the oral, gastric,
200 and small-intestine digestions were simulated with digestive fluids added sequentially to the
201 sample in a conical 50-mL tube and mixed by head-over-heels agitation at 50 rpm. All reagents
202 and extracts for *in vitro* digestion were obtained from Sigma-Aldrich. Bovine serum albumin

203 (A7906) and commercial porcine α -amylase (A3176-1MU), mucin (M1778), pepsin (P7000),
204 pancreatin (P7545), pancreatic lipase (L3126), and bile (B8631) extracts were used to recreate
205 the composition of the digestive fluids (Versantvoort, Oomen, Kamp, Rompelberg, & Sips,
206 2005).

207 The cheeses were cut to a standardized surface-to-volume ratio of 20 cm^{-1} (i.e. 3-mm cubes)
208 (Lamothe et al., 2012). Each digestion tube contained 4.5 g of cheese and 2.5 g of 4-mm glass
209 beads to ensure thorough mixing of the samples. Oral (6 mL), gastric (12 mL), and intestinal
210 (20 mL) fluids were added after 0, 5, and 120 min, respectively. The fluids for the intestinal
211 phase (6:3:1 ratio of duodenal, bile, and 1 M NaHCO_3 solutions, respectively) were premixed for
212 5 min before being added to the tubes. To compensate for the buffering effect of the cheese,
213 250 μL of 5N HCl was added to each tube at the beginning of the gastric phase to maintain
214 acidic conditions, and 6.776 g of NaHCO_3 was added to 700 mL of the intestinal fluid premix.
215 The duration of the intestinal phase was set to 180 min, for a total digestion time of 300 min.
216 Samples for analyses were taken after 5, 60, 120, 150, 180, 240, and 300 min. One digestion tube
217 was taken at every sampling time, analyzed, and then discarded.

218 Cheese disintegration was quantified using the matrix degradation index (MDI), obtained
219 from the undigested cheese fraction retained by a metallic sieve ($1.5 \times 1.5 \text{ mm}$), as previously
220 described (Lamothe et al., 2012). The solids were washed twice with 5 mL of unused digestive
221 fluids (saliva, gastric, or intestinal fluid, depending on the moment of sampling) at 37°C . The
222 sieve with the retained solids was drained and blotted on a filter paper cone for 10 min to remove
223 any remaining fluid. The solids were transferred to a pre-weighed aluminum dish and dried in a
224 forced-air oven at 100°C for 12 h. The dry solids were weighed, the mass of the glass beads was
225 deducted, and the remaining amount of solids was used to obtain the MDI, using Eq. (1):

226

$$227 \quad \text{MDI}(\%) = 100 \times \frac{CS_0 - CS_t}{CS_0} \quad (1)$$

228

229 where CS_0 is the mass of cheese solids originally present in the digestion tube, and CS_t is the
230 mass of cheese solids remaining at time t .

231 The extent of lipolysis was measured using a non-esterified fatty acid (NEFA) enzymatic kit
232 (Roche Diagnostics, Indianapolis, IN, USA). The drained liquid from the MDI samples was
233 diluted 100-fold with a solution of ethanol and Triton X-100 (Sigma Aldrich; 6 mL and 5.7 g,
234 respectively, completed to 100 mL with distilled water) to solubilize the fatty acids and halt
235 lipolysis (Lamothe et al., 2012). The assay was carried out according to the instructions provided
236 with the kit. Absorbance was measured at 546 nm with a DU800 spectrophotometer (Beckman
237 Coulter, Fullerton, CA, USA). Oleic acid was used as the calibration standard. The NEFAs were
238 expressed as mg g^{-1} of milk fat present in the cheese sample, assuming an average molecular
239 weight of 247 g mol^{-1} for milk fatty acids (Lamothe et al., 2012). Lipolysis was expressed as the
240 percentage of fatty acids released from the theoretical maximum of 66% [i.e. pancreatic lipase
241 cleaves only sn_1 - and sn_3 -fatty acids from the triglyceride molecule (Jones & Kubow, 2006)].

242

243 *2.7. Statistical analysis*

244

245 All analyses were repeated three times. Data were analyzed for statistical differences by a
246 two-way analysis of variance (ANOVA) in a split-plot array with the calcium level nested in the
247 main plot and ripening in the sub-plot. Multiple comparisons were done using least significant

248 difference (LSD) with a significance level of $P \leq 0.01$. For the *in vitro* digestion experiments,
249 data were analyzed using a three-way ANOVA in a split-split-plot with the digestion time in the
250 sub-sub-plot. All statistical analyses were carried out with SAS-Server Interface (version 2.0.4;
251 SAS Institute Inc., Cary, NC, USA).

252

253 **3. Results and discussion**

254

255 *3.1. Cheese appearance and composition*

256

257 All freshly made cheeses were similar in appearance to commercial fresh Cheddar cheese.
258 During the salting step, the temperature of the curds salted with the highest level of $\text{CaCl}_2 \cdot 2\text{H}_2\text{O}$
259 increased $6 \pm 2^\circ\text{C}$ relative to the control because of the heat released during $\text{CaCl}_2 \cdot 2\text{H}_2\text{O}$
260 solubilization. The temperature change could be avoided by using a concentrated solution of
261 CaCl_2 instead of using the dry salt. After pressing, the curds had begun to bond, and all the
262 cheese blocks could be easily handled. The very high-calcium cheese was slightly oily to the
263 touch, possibly because of the warming of the curd during the salting step. After 1 week, all the
264 cheeses could be cut easily with a wire cutter to divide them into separate portions for the
265 different ripening durations. No differences were observed after thawing for any of the
266 experimental cheeses except the very high-calcium one ripened for 1 week, which was found to
267 have weakened milled-curd junctions when handled.

268 The composition of the experimental cheeses is presented in Table 2. The moisture level
269 decreased as the calcium level increased ($P < 0.0001$), owing mainly to the osmotic pressure
270 caused by the excess $\text{CaCl}_2 \cdot 2\text{H}_2\text{O}$ (Table 1). This effect was noticeable during the pressing of the

271 cheeses, when more whey was expelled from the molds of the calcium-enriched cheeses. The
272 lower moisture levels led to a relative increase in protein in the calcium-enriched cheeses
273 ($P < 0.0001$), but the protein-to-fat ratio was similar for all the cheeses (0.76 ± 0.03). As
274 expected, ash residue was lowest for the control and increased ($P = 0.0002$) with the amount of
275 $\text{CaCl}_2 \cdot 2\text{H}_2\text{O}$ used during the salting step. Differences for fat content were not statistically
276 significant ($P > 0.05$). Finally, the pH of the cheeses decreased with $\text{CaCl}_2 \cdot 2\text{H}_2\text{O}$ enrichment
277 ($P = 0.001$) owing to H^+ ions released by the interaction of calcium with phosphate and citrate
278 (Philippe, Gaucheron, Le Graet, Michel, & Garem, 2003). No composition changes were
279 observed during ripening.

280 Total calcium and colloidal calcium concentration in experimental cheeses is presented in
281 Table 3. As expected, cheese calcium concentration increased as the calcium level during the
282 salting process increased ($P = 0.0005$). The proportion of colloidal calcium in the control cheese
283 after 1 week of ripening was 62%, with respect to the total calcium, which is within range for a
284 normal Cheddar cheese (Hassan et al., 2004). The addition of $\text{CaCl}_2 \cdot 2\text{H}_2\text{O}$ during the salting step
285 increased the colloidal calcium concentration by as much as twofold relative to the control
286 cheese. Ripening had a slight effect ($P = 0.0499$) on CCP, but the effect was limited to the
287 control cheese, where CCP solubilization during ripening was observed, especially after 4 weeks.
288 The proportion of CCP did not vary during the ripening of the calcium-enriched cheeses, because
289 of calcium oversaturation, preventing CCP solubilization. Based on those results, a more tightly
290 structured protein matrix could be expected as the calcium enrichment level increased (Johnson
291 & Lucey, 2006; Lucey, Johnson, & Horne, 2003).

292 Water-soluble nitrogen evolved differently during the ripening process depending on the
293 calcium level in the cheese, as confirmed by the calcium \times ripening interaction ($P = 0.0022$)

294 observed. As expected, water-soluble nitrogen increased in the control cheese during ripening
295 (O'Mahony et al., 2005), but the increase was slower in the high-calcium cheese, and no increase
296 was observed in the very high-calcium cheese (Table 4). These differences were probably due to
297 higher ionic strength and lower water activity, which reduced the proteolytic activity in the
298 cheeses to which higher amounts of $\text{CaCl}_2 \cdot 2\text{H}_2\text{O}$ had been added during the salting step (Upreti,
299 Metzger, & Hayes, 2006). Proteolysis progression in Cheddar cheeses has been reported to be
300 higher with increased moisture in the non-fat substance (Guinee et al., 2000). In this study, such
301 ratios were 0.565, 0.525, and 0.487 for the control, high-calcium, and very high-calcium cheeses,
302 so the trend in their proteolytic activity (Table 4) is in agreement with their moisture in the non-
303 fat substance.

304

305 *3.2. Cheese texture*

306

307 Cheese texture was analyzed using TPA data from a two-compression cycle. The results for
308 TPA properties are presented in Table 5. Cheese hardness was influenced by added calcium and,
309 for the very high-calcium cheese, by ripening duration ($P = 0.0029$). Hardness increased as the
310 level of calcium in the cheese increased, mainly because of the loss of moisture during the
311 pressing step, which resulted in a drier matrix that exerted a higher resistance to compression
312 (Creamer & Olson, 1982), as well as because of the higher CCP content, which increased the
313 strength of the protein matrix (Lucey et al., 2003). The effect of ripening on hardness was not
314 statistically significant for the control and high-calcium cheeses but was statistically significant
315 for the very high-calcium cheese after 4 weeks. Normally, Cheddar cheese is expected to soften
316 during the first 4 weeks after production, mainly because of CCP solubilization and, to a lesser

317 extent, proteolysis (Creamer & Olson, 1982; Guinee et al., 2000; O'Mahony et al., 2005).
318 However, no such effect was observed in the experimental cheeses; hardness remained stable in
319 all the cheeses except the very high-calcium one, which was markedly harder after 4 weeks of
320 ripening. This greater hardness observed after four weeks may result from the gradual fusion of
321 milled curd during ripening. A high concentration of calcium has been suggested to interfere
322 with the fusion of milled curd during pressing (Ong et al., 2013) by increasing curd surface
323 dehydration and rigidity. The negative effect of calcium of curd bonding is, however, expected to
324 decrease during ripening due to the gradual elimination of moisture and salt gradients.

325 Springiness, which is the height recovery ratio between the two compressions (Bourne,
326 1978), was also dependent on the calcium level in the cheeses ($P = 0.0002$). In general, sample-
327 height recovery was almost total, although it was slightly lower in the control than in the high-
328 calcium and very high-calcium cheeses. A significant but small difference between the two
329 calcium-enriched cheeses was also detected. It seems that calcium, mainly as CCP, had a
330 structuring effect that yielded a matrix that was more capable of recovery after compression.
331 Perhaps a higher strain would have ended in an abrupt fracture from which the samples would
332 not have recovered, but this was not the case under the test parameters used.

333 Finally, cohesiveness, which represents the applied-work ratio between the second and first
334 compressions (Bourne, 1978), was statistically similar for all the cheeses, meaning that the
335 strength of the internal bonds of the food was reduced proportionally after the first compression
336 for all the cheeses. Nevertheless, a trend towards a more cohesive matrix with higher calcium
337 levels was observed.

338

339 3.3. *Cheese microstructure*

340

341 Scanning electron micrographs of the cheeses after 4 weeks of ripening are shown in Fig. 1.
342 The images show the protein matrix and the voids once occupied by milk fat, which was
343 removed during sample preparation. The control cheese had a continuous protein matrix
344 containing individual and coalesced milk-fat globules, in keeping with previous observations for
345 a young Cheddar cheese of similar composition (Lamothe et al., 2012; Mistry & Anderson,
346 1993). The distribution of the fat globules changed when higher levels of $\text{CaCl}_2 \cdot 2\text{H}_2\text{O}$ were
347 added at the salting step. As the calcium level increased, the aggregation of the milk-fat globules
348 seemed to increase, producing larger and irregular fat aggregates within the protein matrix
349 (Fig. 1). Also as the calcium level increased, the protein matrix appeared stringier than it was in
350 the control. In Cheddar cheese, protein fibers align in stringy patterns during cheddaring and,
351 without losing their oriented nature, swell with the available moisture, slowly evolving into a
352 compact uniform mass during ripening (Everett, 2007; Kalab & Emmons, 1978). Hence, the
353 greater moisture loss when higher amounts of $\text{CaCl}_2 \cdot 2\text{H}_2\text{O}$ were added limited the amount of
354 water available for the hydration of protein fibers. The more compact protein matrix resulting
355 from such water loss allowed milk fat to aggregate further into larger and more continuous
356 reservoirs, as seen in the very high-calcium cheese (Fig. 1).

357 Confocal laser micrographs show the distribution of protein (represented in red) and fat
358 (represented in green) in the different cheeses (Fig. 2). As with the scanning electron
359 micrographs, the confocal laser micrographs were obtained from the cheeses ripened for
360 4 weeks. The superimposed protein and fat images show the fat-embedded protein matrix
361 (Fig. 2). The control cheese had a more continuous protein matrix containing small fat reservoirs.

362 As the calcium level increased, the uniformity of the para-casein matrix with respect to fat
363 dispersion seemed to decrease. In the control cheese, fat was more uniformly dispersed in
364 individual globules or in small aggregates, which were larger in the high-calcium cheese (Fig. 2).
365 In the very high-calcium cheese, the fat aggregates were less regular in shape and were branched,
366 unlike those present in the other cheeses. These differences appear to have been caused by the
367 drastic water loss of the protein matrix. Hence, the irregular shape and large size of the fat
368 reservoirs in the very high-calcium cheese occurred because the milk fat adopted the stretched
369 arrangement of the protein, as was also observed in the scanning electron micrographs (Fig. 1).
370 The slight linear orientation was produced during the cheddaring step (Hall & Creamer, 1972;
371 Kalab & Emmons, 1978; Taranto, Wan, Chen, & Rhee, 1979) and the pressing step (Auty et al.,
372 2001).

373

374 *3.4. In vitro digestion of cheese*

375

376 Physical disintegration during *in vitro* digestion progressed differently ($P < 0.0001$)
377 depending on the calcium level in the cheeses (Fig. 3a). When measured at the end of the oral
378 phase (5 min), MDI values were higher for the calcium-enriched cheeses than those obtained for
379 the control ($P = 0.0002$) (Fig. 3a). These higher values may be explained by the brittle texture of
380 the cheeses salted with calcium chloride. Although the conditions used for texture analysis did
381 not allow direct determination of brittleness (no fracture), high brittleness of calcium-enriched
382 cheeses could be visually observed during sample preparation for *in vitro* digestion. Cheese
383 crumbs most likely became detached in the simulated saliva and were lost through the sieve. In
384 contrast, the control did not yield fine particles during this stage of digestion. A similar study,

385 which used the same *in vitro* digestion model, suggested that the brittleness of aged Cheddar
386 cheese was responsible for MDI values that were three times higher after the oral phase in
387 comparison with the values for less-brittle mild and low-fat Cheddar cheeses (Lamothe et al.,
388 2012). Towards the end of the gastric phase, the cheese with very high calcium had the lowest
389 MDI ($P < 0.0001$). Surprisingly, the high-calcium cheese had the highest MDI after 120 min
390 ($P < 0.0001$; Fig. 3a), despite having a lower moisture-to-protein ratio (1.37) than the control had
391 (1.62). Within similar matrices, higher moisture-to-protein ratios would be expected to accelerate
392 disintegration by enabling faster diffusion (e.g. of digestive enzymes or calcium ions) through
393 the cheese owing to an increase in the relative pore width of the protein matrix (Guinee & Fox,
394 2004). During the gastric phase, the digestion of dislodged particles arising from the weaker
395 milled-curd bonding could explain the faster disintegration of the high-calcium cheese in
396 comparison with the control. The resistance of the very high-calcium cheese could be due to its
397 appreciably low moisture-to-protein ratio (1.24), which slowed down the rate at which the cheese
398 particles disintegrated. After 30 min of the intestinal phase had passed, the cheeses had
399 disintegrated considerably, although the very high-calcium cheese was more resistant
400 ($P < 0.0001$) than the others (Fig. 3a). The large increase after the addition of intestinal fluids was
401 due to the action of trypsin and chymotrypsin (contained in the pancreatin extract), which rapidly
402 completed the hydrolysis of the hydrated and exposed protein matrix. After 300 min of *in vitro*
403 digestion, at the end of the intestinal phase, the control and the high-calcium cheeses had
404 disintegrated completely (MDI values of 99.6% and 99.2% \pm 0.5%, respectively). In contrast, the
405 very high-calcium cheeses reached a lower MDI (94.6% \pm 0.5%) than the other cheeses
406 ($P < 0.0001$), all ripening conditions combined. For the very high-calcium cheeses, the residue

407 recovered for the MDI test was highly hydrated but still represented a portion of the solids
408 contained in the original sample.

409 Ripening had a small but statistically significant effect on reducing MDI values ($P = 0.0018$)
410 during the *in vitro* digestion of the experimental cheeses (Fig. 3b). After 120 and 150 min of
411 digestion (i.e. at the end of the gastric phase and 30 min into the intestinal phase, respectively),
412 the cheeses ripened for 4 weeks were slightly more resistant to disintegration (i.e. MDI variations
413 below 5%) than were those ripened for 1 or 2 weeks ($P < 0.0001$). As previously mentioned, this
414 difference could be due to the better bonding of the milled curds after 4 weeks of ripening,
415 although no effect was observed after the digestion was completed ($P > 0.5$).

416 Before the addition of the simulated intestinal fluids, the NEFAs detected in the chyme were
417 lower than 0.01%. No lipases were used in the oral or gastric phase, so lipolysis did not occur
418 until the intestinal fluids were added. Once the intestinal phase began, lipolysis increased during
419 digestion, depending on the calcium level in the cheese ($P = 0.0005$; Fig. 4). Cheese ripening had
420 no significant effect on lipolysis ($P > 0.05$). During the first 30 min under intestinal conditions,
421 fatty-acid release was abundant for all the cheeses owing to the rapid lipolysis of the free milk fat
422 that had detached from the cheese matrices during the gastric phase and during the rapid
423 degradation at the beginning of the intestinal phase. This observation is in accordance with a
424 previous study with full-fat Cheddar cheeses using the same digestion model, where at least 60%
425 of the oil was free after only 30 min of intestinal digestion (Lamothe et al., 2012). The high
426 amount of free fat was readily accessible to the pancreatic lipase in the chyme. Lipolysis
427 progressed faster for the calcium-enriched cheeses than for the control ($P < 0.0001$), and the
428 effect was consistent for the first 90 min of intestinal digestion. During the last 90 min of *in vitro*
429 digestion, lipolysis progression slowed down and seemed to reach a plateau. The final lipolysis

430 rates after 300 min of digestion were 73.6%, 77.9%, and 72.5% (standard error of the mean =
431 1.61%) for the control, high-calcium, and very high-calcium cheeses, respectively, with a
432 statistical difference between the last two ($P = 0.0148$).

433 Calcium has been shown to increase lipolysis rates, an effect that can be explained by the
434 depletion of free fatty acids at the lipid–water interface. Calcium soaps are produced with free
435 fatty acids in the vicinity of neutral pH, and they precipitate under intestinal pH conditions,
436 freeing the lipid–water interface so that lipase may access its substrate (Devraj et al., 2013; Hu et
437 al., 2010). In the very high-calcium cheese, some fat may have still been trapped in the cheese
438 matrix residue towards the end of digestion and would have been protected from the pancreatic
439 lipase. The effect of calcium on lipolysis may also be attributed to a change in cheese
440 microstructure that increases free fat release from the matrix during digestion. The calcium-
441 enriched matrices presented a high degree of fat aggregation interconnecting the fat reservoirs in
442 comparison with the control (Figs. 1 and 2). During *in vitro* digestion, the molten fat (at 37°C)
443 would have readily exited the partially digested matrix, emptying into the chyme and enabling
444 faster lipolysis as free fat. This phenomenon would explain the high lipolysis rates even if
445 physical disintegration of the protein matrix was not complete.

446 At the end of digestion, lipolysis did not reach completion (i.e. 100% of the potential
447 NEFAs), probably because the *in vitro* system used does not mimic nutrient absorption and thus
448 reaction products accumulate in the chyme, eventually halting the enzymatic reaction.
449 Nonetheless, the results are comparable to those obtained for Cheddar cheese with the same *in*
450 *vitro* digestion model (Lamothe et al., 2012).

451

452 4. Conclusions

453

454 Adding calcium chloride during the salting step of cheese manufacture had a significant
455 impact on cheese structure and the behavior during *in vitro* digestion. Calcium chloride
456 enrichment increased ionic strength and pH. It also reduced the moisture content of the cheeses
457 during the pressing stage. Such changes resulted in modified texture parameters and
458 microstructure.

459 Under the conditions set for this study, short-term ripening had only a limited effect on
460 cheese texture and digestion, and that effect differed, depending on the calcium level in the
461 cheese. Although short-term ripening of the cheeses caused variations in the extent of proteolysis
462 and the solubilization of CCP, the impact of such processes on cheese structure was lower than
463 expected, and the cheeses did not show any major changes in texture properties during the
464 ripening period, explaining the similarities observed on MDI and lipolysis during *in vitro*
465 digestion of the different cheeses. Higher calcium levels led to faster lipolysis during the first
466 half of the intestinal digestion, possibly by enhancing lipase activity. The protective effect of the
467 matrix on lipolysis was observed for the very-high calcium cheese towards the end of the
468 digestion, where less NEFA were detected even in the presence of higher calcium levels, when
469 compared to the other cheeses.

470 This study revealed that enrichment of Cheddar curds with CaCl_2 during salting produced
471 major modifications to the final cheese matrix by modifying the composition, structure and
472 physicochemical evolution during short term ripening. Such modifications affected the behavior
473 on the cheese matrices during *in vitro* digestion, and are clear example that the food matrix and
474 microstructure could help control the release of lipid nutrients from cheese. This study also

475 provides insight into technological processes that can be used to achieve such nutrient
476 modulation. Further work on cheeses with similar composition and structure are being carried
477 out to better understand the net effect of calcium on fatty acid bioaccessibility. Eventually, the
478 findings of this study could lead to the discovery of novel nutritional aspects that could be
479 adapted for the food industry to, among other things, control nutrient release, deliver bioactive
480 molecules, and build evidence to substantiate health claims.

481

482 **Acknowledgements**

483

484 The authors wish to thank Gaetan Bélanger for his help with cheese manufacture, Sophie
485 Lamothe and Marie-France Morissette for their valuable assistance with the *in vitro* digestion
486 model, and Milos Kalab, Shea Miller, and Ann-Fook Yang for their help with microscope
487 imaging and interpretation. The financial support of NSERC, NOVALAIT, MAPAQ, FQRNT,
488 and AAFC is acknowledged.

References

- AOAC.(1995a). Method 920.123, Nitrogen in cheese. In P. Cunniff (Ed.), *Official methods of analysis of AOAC International: Vol. 2* (16th edn.) (pp. 33.7.12). Gaithersburg, MD, USA: AOAC International.
- AOAC.(1995b). Method 933.05, Fat in cheese. In P. Cunniff (Ed.), *Official methods of analysis of AOAC International: Vol. 2* (16th edn.) (pp. 33.7.17). Gaithersburg, MD, USA: AOAC International.
- Armand, M., Pasquier, B., André, M., Borel, P., Senft, M., Peyrot, J., Salducci, J., Portugal, H., Jaussan, V., & Lairon, D. (1999). Digestion and absorption of 2 fat emulsions with different droplet sizes in the human digestive tract. *American Journal of Clinical Nutrition*, 70, 1096–1106.
- Auty, M. A. E., Twomey, M., Guinee, T. P., & Mulvihill, D. M. (2001). Development and application of confocal scanning laser microscopy methods for studying the distribution of fat and protein in selected dairy products. *Journal of Dairy Research*, 68, 417–427.
- Bourne, M. C. (1978). Texture profile analysis. *Food Technology*, 32, 62–66, 72.
- Canadian Dairy Commission. (2015). Typical composition of Cheddar cheese. Retrieved 2015-05-10, from <http://www.milkingredients.ca/index-eng.php?id=174>
- Christensen, T. M. I. E., Bech, A.-M., & Werner, H. (1991). Methods for crude fractionation (extraction and precipitation) of nitrogen components in cheese. *Bulletin of the International Dairy Federation*, 261, 4–9.
- Clemente, G., Mancini, M., Nazzaro, F., Lasorella, G., Riviaccio, A., Palumbo, A. M., Rivellese, A. A., Ferrara, L., & Giacco, R. (2003). Effects of different dairy products on postprandial lipemia. *Nutrition Metabolism and Cardiovascular Diseases*, 13, 377–383.
- Creamer, L. K., & Olson, N. F. (1982). Rheological evaluation of maturing Cheddar cheese. *Journal of Food Science*, 47, 631–636, 646.
- Devraj, R., Williams, H. D., Warren, D. B., Mullertz, A., Porter, C. J. H., & Pouton, C. W. (2013). *In vitro* digestion testing of lipid-based delivery systems: Calcium ions combine with fatty acids liberated from triglyceride rich lipid solutions to form soaps and reduce

- the solubilization capacity of colloidal digestion products. *International Journal of Pharmaceutics*, 441, 323–333.
- Ellis, P. R., Kendall, C. W., Ren, Y., Parker, C., Pacy, J. F., Waldron, K. W., & Jenkins, D. J. (2004). Role of cell walls in the bioaccessibility of lipids in almond seeds. *American Journal of Clinical Nutrition*, 80, 604-613.
- Everett, D. W. (2007). Microstructure of natural cheeses. In A. Y. Tamime (Ed.), *Structure of dairy products* (pp. 170–209). Oxford, UK: Blackwell Publishing Ltd.
- Failla, M. L., & Chitchumronchokchai, C. (2005). *In vitro* models as tools for screening the relative bioavailabilities of provitamin A carotenoids in foods. HarvestPlus Technical Monograph Series 3. Washington, DC, USA: HarvestPlus.
- Favé, G., Coste, T. C., & Armand, M. (2004). Physicochemical properties of lipids: New strategies to manage fatty acid bioavailability. *Cellular and Molecular Biology*, 50, 815–831.
- Guinee, T. P., Auty, M. A. E., & Fenelon, M. A. (2000). The effect of fat content on the rheology, microstructure and heat-induced functional characteristics of Cheddar cheese. *International Dairy Journal*, 10, 277–288.
- Guinee, T. P., & Fox, P. F. (2004). Salt in cheese: Physical, chemical and biological aspects. In P. F. Fox, P. L. H. McSweeney, T. M. Cogan, & T. P. Guinee (Eds.), *Cheese: Chemistry, physics and microbiology: Vol. 1, General aspects* (3rd edn.) (pp. 207–259). London, UK: Elsevier Academic Press.
- Hall, D. M., & Creamer, L. K. (1972). A study of the sub-microscopic structure of Cheddar, Cheshire and Gouda cheese by electron microscopy. *New Zealand Journal of Dairy Science and Technology*, 7, 95–102.
- Hassan, A., Johnson, M. E., & Lucey, J. A. (2004). Changes in the proportions of soluble and insoluble calcium during the ripening of Cheddar cheese. *Journal of Dairy Science*, 87, 854–862.
- Hornero-Méndez, D., & Mínguez-Mosquera, M. I. (2007). Bioaccessibility of carotenes from carrots: Effect of cooking and addition of oil. *Innovative Food Science & Emerging Technologies*, 8, 407-412.

- Hu, M., Li, Y., Decker, E. A., & McClements, D. J. (2010). Role of calcium and calcium-binding agents on the lipase digestibility of emulsified lipids using an *in vitro* digestion model. *Food Hydrocolloids*, *24*, 719–725.
- Hur, S. J., Lim, B. O., Decker, E. A., & McClements, D. J. (2011). *In vitro* human digestion models for food applications. *Food Chemistry*, *125*, 1–12.
- Johnson, M. E., & Lucey, J. A. (2006). Calcium: A key factor in controlling cheese functionality. *Australian Journal of Dairy Technology*, *61*, 147–153.
- Jones, P. J. H., & Kubow, S. (2006). Lipids, sterols, and their metabolites. In M. E. Shils, M. Shike, A. C. Ross, B. Caballero, & R. J. Cousins (Eds.), *Modern nutrition in health and disease* (10th edn.) (pp. 92–122). Baltimore, MD, USA: Lippincott Williams & Wilkins.
- Kalab, M., & Emmons, D. B. (1978). Milk gel structure. IX. Microstructure of cheddared curd. *Milchwissenschaft*, *33*, 670–673.
- Kasprzak, K., Wendorff, W. L., & Chen, C. M. (1994). Freezing qualities of Cheddar-type cheeses containing varied percentages of fat, moisture, and salt. *Journal of Dairy Science*, *77*, 1771–1782.
- Klein, S., Cohn, S. M., & Alpers, D. H. (2006). Alimentary tract in nutrition. In M. E. Shils, M. Shike, A. C. Ross, B. Caballero, & R. J. Cousins (Eds.), *Modern nutrition in health and disease* (10th edn.) (pp. 1115–1142). Baltimore, MD, USA: Lippincott Williams & Wilkins.
- Lamothe, S., Corbeil, M.-M., Turgeon, S. L., & Britten, M. (2012). Influence of cheese matrix on lipid digestion in a simulated gastro-intestinal environment. *Food & Function*, *3*, 724–731.
- Lawrence, R. C., Gilles, J., Creamer, L. K., Crow, V. L., Heap, H. A., Honoré, C. G., Johnston, K. A., & Samal, P. K. (2004). Cheddar cheese and related dry-salted cheese varieties. In P. F. Fox, P. L. H. McSweeney, T. M. Cogan, & T. P. Guinee (Eds.), *Cheese: Chemistry, physics and microbiology: Vol. 2, Major cheese groups* (3rd edn.) (pp. 71–102). London, UK: Elsevier Academic Press.
- Lopez, C., & Gaucheron, F. (2008). Nutritional quality of dairy products: Effects of lipid composition and suprastructure and role played by the other constituents of the matrix on the digestion and absorption of fatty acids. *Sciences des Aliments*, *28*, 106–116.

- Lorenzen, J. K., Nielsen, S., Holst, J. J., Tetens, I., Rehfeld, J. F., & Astrup, A. (2007). Effect of dairy calcium or supplementary calcium intake on postprandial fat metabolism, appetite, and subsequent energy intake. *American Journal of Clinical Nutrition*, *85*, 678–687.
- Lucey, J. A., & Fox, P. F. (1993). Importance of calcium and phosphate in cheese manufacture: A review. *Journal of Dairy Science*, *76*, 1714–1724.
- Lucey, J. A., Johnson, M. E., & Horne, D. S. (2003). Invited review: Perspectives on the basis of the rheology and texture properties of cheese. *Journal of Dairy Science*, *86*, 2725–2743.
- McClements, D. J., Decker, E. A., & Park, Y. (2009). Controlling lipid bioavailability through physicochemical and structural approaches. *Critical Reviews in Food Science and Nutrition*, *49*, 48–67.
- Metzger, L. E., & Mistry, V. V. (1994). A new approach using homogenization of cream in the manufacture of reduced fat Cheddar cheese. 1. Manufacture, composition, and yield. *Journal of Dairy Science*, *77*, 3506–3515.
- Metzger, L. E., & Mistry, V. V. (1995). A new approach using homogenization of cream in the manufacture of reduced fat Cheddar cheese. 2. Microstructure, fat globule distribution, and free oil. *Journal of Dairy Science*, *78*, 1883–1895.
- Michalski, M.-C., Briard, V., Desage, M., & Geloën, A. (2005). The dispersion state of milk fat influences triglyceride metabolism in the rat. A $^{13}\text{CO}_2$ breath test study. *European Journal of Nutrition*, *44*, 436–444.
- Michalski, M.-C., Camier, B., Gassi, J.-Y., Briard-Bion, V., Leconte, N., Famelart, M.-H., & Lopez, C. (2007). Functionality of smaller vs control native milk fat globules in Emmental cheeses manufactured with adapted technologies. *Food Research International*, *40*, 191–202.
- Michalski, M.-C., Michel, F., & Geneste, C. (2002). Appearance of submicronic particles in the milk fat globule size distribution upon mechanical treatments. *Lait*, *82*, 193–208.
- Mistry, V. V., & Anderson, D. J. (1993). Composition and microstructure of commercial full-fat and low-fat cheeses. *Food Structure*, *12*, 259–266.
- O'Mahony, J. A., Lucey, J. A., & McSweeney, P. L. H. (2005). Chymosin-mediated proteolysis, calcium solubilization, and texture development during the ripening of Cheddar cheese. *Journal of Dairy Science*, *88*, 3101–3114.

- O'Mahony, J. A., McSweeney, P. L. H., & Lucey, J. A. (2006). A model system for studying the effects of colloidal calcium phosphate concentration on the rheological properties of Cheddar cheese. *Journal of Dairy Science*, *89*, 892–904.
- Philippe, M., Gaucheron, F., Le Graet, Y., Michel, F., & Garem, A. (2003). Physicochemical characterization of calcium-supplemented skim milk. *Lait*, *83*, 45–59.
- Rémillard, N., & Britten, M. (2011). Quantitative determination of micellar calcium in milk and cheese using acid-base titration. *Milchwissenschaft*, *66*, 137–140.
- Ruby, M. V., Schoof, R., Brattin, W., Goldade, M., Post, G., Harnois, M., Mosby, D. E., Casteel, S. W., Berti, W., Carpenter, M., Edwards, E., & Chappell, W. (1999). Advances in evaluating the oral bioavailability of inorganics in soil for use in human health risk assessment. *Environmental Science & Technology*, *33*, 3697–3705.
- Singh, H., Ye, A., & Horne, D. (2009). Structuring food emulsions in the gastrointestinal tract to modify lipid digestion. *Progress in Lipid Research*, *48*, 92–100.
- Taranto, M. V., Wan, P. J., Chen, S. L., & Rhee, K. C. (1979). Morphological, ultrastructural and rheological characterization of Cheddar and Mozzarella cheese. *Scanning Electron Microscopy*, *1979*, 273–277.
- Tunick, M. H. (2000). Rheology of dairy foods that gel, stretch, and fracture. *Journal of Dairy Science*, *83*, 1892–1898.
- Turgeon, S. L., & Rioux, L.-E. (2011). Food matrix impact on macronutrients nutritional properties. *Food Hydrocolloids*, *25*, 1915–1924.
- Upreti, P., Metzger, L. E., & Hayes, K. D. (2006). Influence of calcium and phosphorus, lactose, and salt-to-moisture ratio on Cheddar cheese quality: Proteolysis during ripening. *Journal of Dairy Science*, *89*, 444–453.
- Van Wey, A. S., Cooksonb, A. L., Roy, N. C., McNabb, W. C., Soboleva, T. K., Wieliczkoa, R. J., & Shortena, P. R. (2014). A mathematical model of the effect of pH and food matrix composition on fluid transport into foods: An application in gastric digestion and cheese brining. *Food Research International*, *57*, 34–43.
- Versantvoort, C. H. M., Oomen, A. G., Van de Kamp, E., Rompelberg, C. J. M., & Sips, A. J. A. M. (2005). Applicability of an in vitro digestion model in assessing the bioaccessibility of mycotoxins from food. *Food and Chemical Toxicology*, *43*, 31–40.

Figure captions

Fig. 1. Scanning electron micrographs of control, high-calcium, and very high-calcium cheeses. Arrows indicate examples of a) a space occupied by an individual milk-fat globule, b) an intact protein matrix, c) a space occupied by partially coalesced milk-fat globules, d) a dehydrated protein matrix, and e) a space occupied by large fat reservoirs. Bar = 10 μm .

Fig. 2. Confocal laser micrographs of control, high-calcium, and very high-calcium cheeses. Green and red channels represent fat and protein, respectively. Overlapping channels (top images) show the distribution of fat and protein within the cheese matrix. Bar = 40 μm .

Fig. 3. Matrix degradation index values during the *in vitro* digestion of a) cheeses with different calcium levels (all ripening times combined) and b) cheeses ripened for 1, 2, or 4 weeks (all calcium levels combined). The first measurement was done after the oral phase was completed (5 min). Digestions carried out in triplicate. Standard error of the mean = 0.51%.

Fig. 4. Evolution of lipolysis during the intestinal phase of the *in vitro* digestion of control, high-calcium, and very high-calcium cheeses. Digestions carried out in triplicate. Standard error of the mean = 1.61%. NEFA, non-esterified fatty acids.

Table 1

Experimental conditions used in the salting step for Cheddar-type cheeses.

Cheese calcium level	NaCl (mass %)	CaCl ₂ ·2H ₂ O (mass %)	Ca added (g kg ⁻¹ curd)
Control	1.80	0	0
High-calcium	1.80	1.47	4
Very high-calcium	1.80	4.40	12

Table 2Composition of a typical fresh Cheddar cheese and the experimental Cheddar cheeses.^a

Cheese	Moisture (%)	Protein (%)	Fat (%)	Ash (%)	pH
Typical ^b	37	25	33	4	5.10
Control	38.6 ^c	23.8 ^a	32.8 ^a	3.30 ^a	5.15 ^c
High-calcium	35.4 ^b	25.8 ^b	32.6 ^a	3.92 ^b	5.10 ^b
Very high-calcium	32.2 ^a	25.9 ^b	33.9 ^a	4.93 ^c	4.99 ^a
SEM ^c	0.1	0.1	0.6	0.12	0.01

^a Different letters within columns denote significantly different means. Only the experimental cheeses were compared.

^b Canadian Dairy Commission, 2015.

^c SEM, standard error of the mean.

Table 3

Total and colloidal calcium (mg g^{-1} protein) of the experimental cheeses after different ripening durations.^a

Cheese	Total calcium ^b	Colloidal calcium after ripening (weeks)		
		1	2	4
Control	25.0 ^a	15.5 ^{a,B}	12.0 ^{a,A,B}	8.6 ^{a,A}
High-calcium	29.6 ^b	28.0 ^{b,A}	26.8 ^{b,A}	26.7 ^{b,A}
Very high-calcium	46.4 ^c	32.8 ^{b,A}	29.3 ^{b,A}	31.9 ^{b,A}

^aDifferent lower case letters denote different means within columns, and different upper case letters denote differences within rows; the overall standard error of the mean was 0.06 for total calcium and 0.15 for colloidal calcium.

^bQuantified by inductively coupled plasma–optical emission spectroscopy.

Table 4

Water-soluble nitrogen (WSN) to total nitrogen (TN) ratio in the experimental cheeses after different ripening durations.^a

Cheese	% WSN TN ⁻¹ after ripening (weeks)		
	1	2	4
Control	8.5 ^{c,A}	9.8 ^{c,B}	12.2 ^{c,C}
High-calcium	5.8 ^{b,A}	5.6 ^{b,A}	7.9 ^{b,B}
Very high-calcium	4.2 ^{a,A}	4.8 ^{a,A}	4.6 ^{a,A}

^aDifferent lower case letters denote different means within columns, and different upper case letters denote differences within rows; the overall standard error of the mean was 0.23.

Table 5Texture of cheeses with different calcium levels.^a

TPA ^b property	Hardness (kPa)			Springiness ^c			Cohesiveness ^c		
	1	2	4	1	2	4	1	2	4
Ripening (weeks)									
Calcium level									
Control	36.9 ^{a,A}	34.7 ^{a,A}	37.0 ^{a,A}	0.805 ^a	0.806 ^a	0.795 ^a	0.644	0.637	0.637
High-calcium	64.6 ^{b,A}	65.9 ^{b,A}	61.0 ^{b,A}	0.875 ^b	0.878 ^b	0.873 ^b	0.669	0.660	0.639
Very high-calcium	77.4 ^{c,A}	78.4 ^{c,A}	85.9 ^{c,B}	0.893 ^c	0.901 ^c	0.896 ^c	0.676	0.673	0.679
SEM ^d	1.3			0.008			0.010		

^aDifferent lower case letters denote differences within columns (i.e. calcium level), whereas different upper case letters denote differences within rows (i.e. ripening duration); no significant differences were detected for cohesiveness.

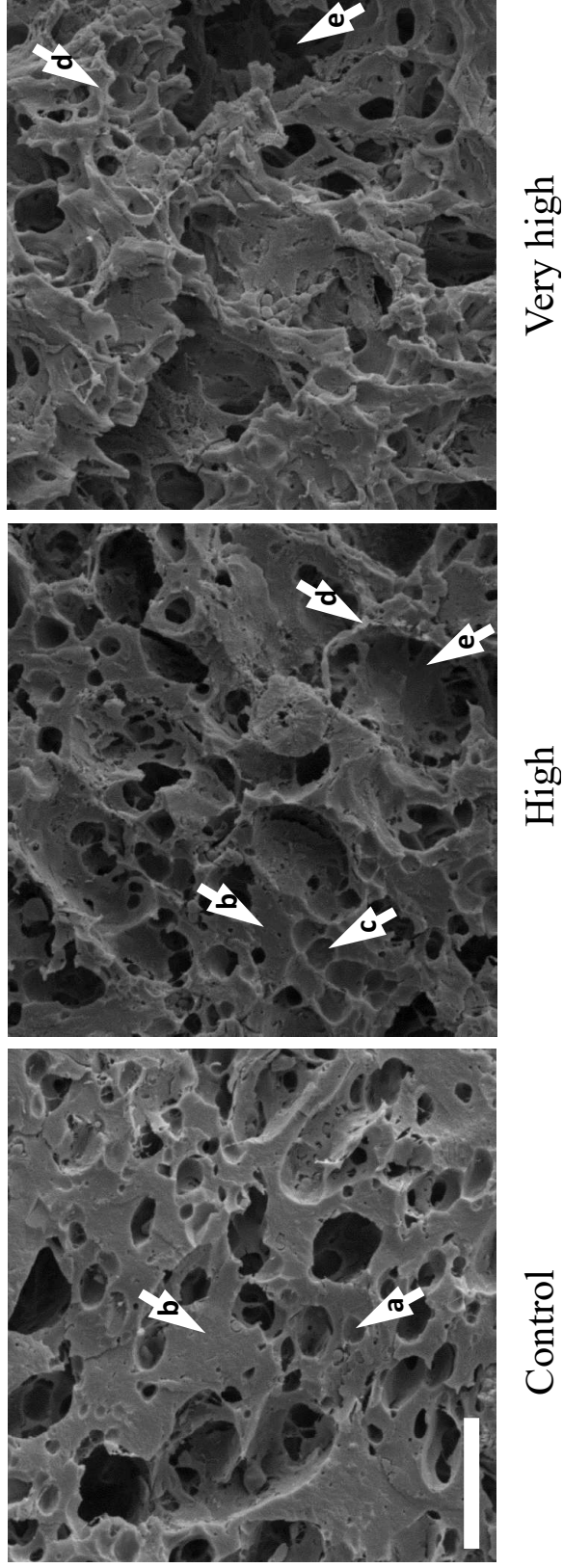
^bTexture profile analysis.

^cProperties expressed without units are dimensionless.

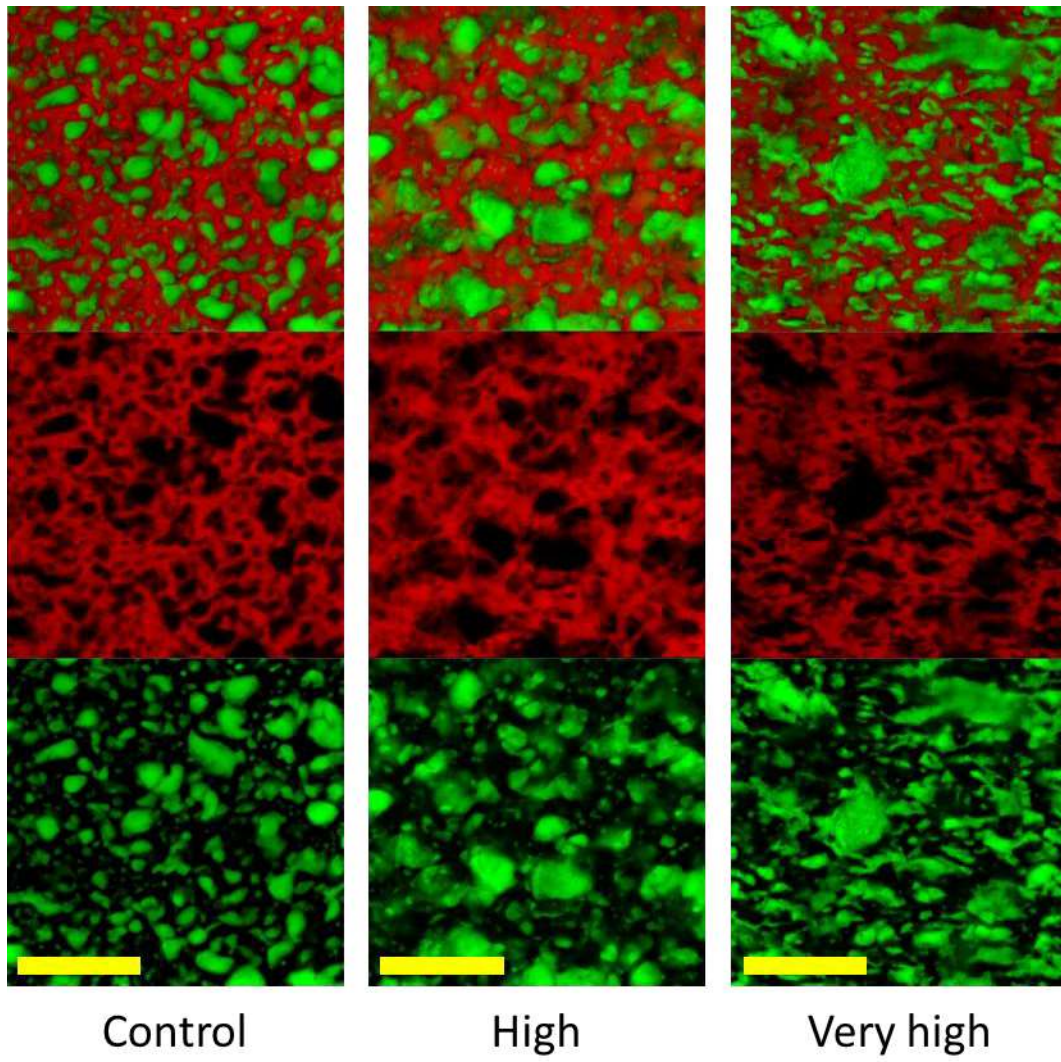
^dStandard error of the mean.

Figure 1

Ayala-Bribiesca et al., Figure 1



Ayala-Bribiesca et al., Figure 2



Ayala-Bribiesca et al., Figure 3

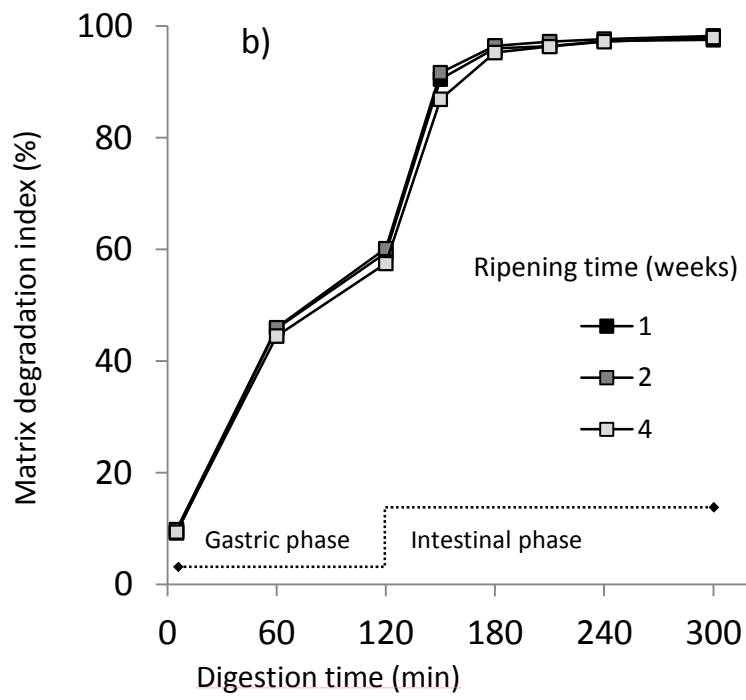
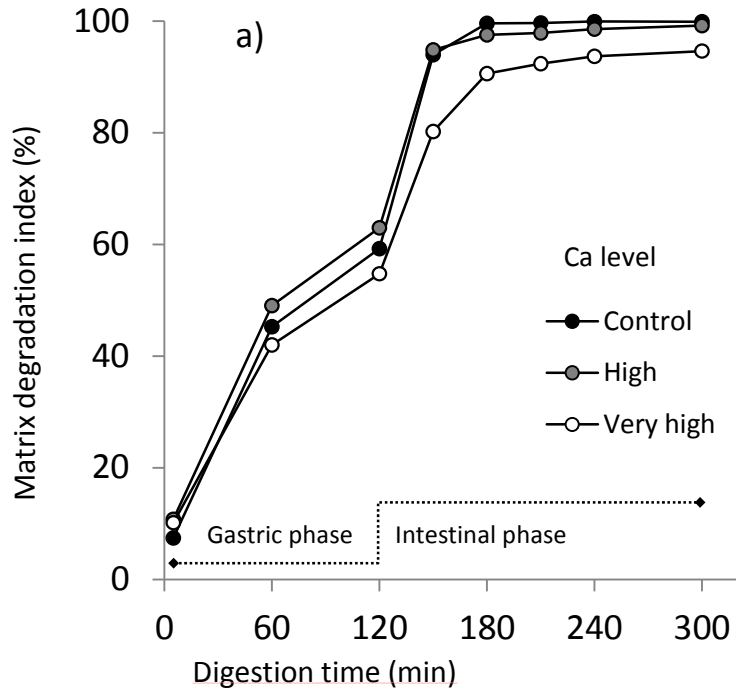


Figure 4

Ayala-Bribiesca et al., Figure 4

